Hindawi Publishing Corporation
International Journal of Optics
Volume 2014, Article ID 534145, 8 pages
http://dx.doi.org/10.1155/2014/534145

Research Article

Enhancement of Photon Absorption on $Ba_xSr_{1-x}TiO_3$ Thin-Film Semiconductor Using Photonic Crystal

Abd. Wahidin Nuayi,[1,2] Husin Alatas,[1] Irzaman S. Husein,[1] and Mamat Rahmat[1]

[1] *Department of Physics, Bogor Agricultural University, Jl. Meranti, Kampus IPB Darmaga, Bogor 16680, Indonesia*
[2] *Department of Physics, University of Gorontalo, Jl. Jend. Sudirman No. 6 Kota Gorontalo, Gorontalo 96128, Indonesia*

Correspondence should be addressed to Husin Alatas; alatas@ipb.ac.id

Received 17 July 2013; Accepted 3 November 2013; Published 9 January 2014

Academic Editor: Augusto Beléndez

Enhancement of photon absorption on barium strontium titanate ($Ba_xSr_{1-x}TiO_3$) thin-film semiconductor for mole fraction x = 0.25, 0.35, 0.45, and 0.55 using one-dimensional photonic crystal with defect was investigated experimentally. The thin film was grown on transparent conductive oxide (TCO) substrate using chemical solution deposition method and annealed at 500°C for 15 hours with increasing rate of 1.6°C/min. From optical characterization in visible spectrum it was found that the average absorption percentages are 92.04%, 83.55%, 91.16%, and 80.12%, respectively. The BST thin film with embedded photonic crystal exhibited a relatively significant enhancement on photon absorption, with increasing value of 3.96%, 7.07%, 3.04%, and 13.33% for the respective mole fraction and demonstrating absorbance characteristic with flat feature. In addition, we also discuss the thin-film properties of attenuation constant and electrical conductivity.

1. Introduction

In solar cell technology, there are some materials that can be used as its base material. Three of them are $CuInSe_2$ (or its alloys such as $CuInS_2$ or $CuInGaSe_2$), CdTe, and amorphous silicon materials. These materials only require one micron thickness to establish an efficient solar cells, due to their high light absorption [1–4]. However, CdTe and $CuInSe_2$ have a bad impact on environment; namely, when the CdTe solar cells are on fire, this cadmium would cause harmful pollution. In laboratory scale, the $CuInSe_2$ material has efficiency above 15%, but it is difficult to control its elements, especially when being produced in larger scale, which implies that it is difficult to produce the associated module even in a laboratory scale [1, 2]. In the mean time, for amorphous silicon material, the related solar cell has been produced in laboratory scale with efficency about 9.5% to 13% [2, 4–7].

There are several other important ferroelectric materials which were studied by many researchers such as $PbTiO_3$, Pb $(Zr_xTi_{1-x})O_3$, $SrBiTaO_3$, $Pb(Mg_{1/3}Nb_{2/3})O_3$, and $BaTiO_3$ which is the basic of $(Ba,Sr)TiO_3$ [8]. Due to its properties, $BaSrTiO_3$ (or BST for short) is a material which has been intensively studied and developed. One of them is in the form of BST thin-film ferroelectric which is used and utilized in electronics such as for light sensor application that can be developed to make solar cells according to optical and electrical characteristics [9, 10].

BST thin film is a material with high dielectric constant, high degree of crystallinity (~800°C), low leakage current, and resistance to high breakdown voltage at Curie's temperature, as well as high capacitance [11, 12]. This thin film can be produced with various methods such as metalorganic chemical vapor deposition (MOCVD) [13], sol-gel [14–17], atomic laser deposition (ALD) [18], hydrothermal synthesis [19], metal organic decomposition (MOD) [20, 21], and chemical solution deposition (CSD) [22–26].

To examine the ability of BST as a material that can be utilized as solar cell, some measurements such as its ability in absorbing photons are required, because antireflective material is more preferred in solar cell system. Photon absorption will affect the efficiency of the associated solar cell. Based on this fact, we have attempted to increase the photon

absorption of a BST thin film grown on transparent conductive oxide (TCO) glass using chemical solution deposition (CSD) method with annealing temperature of 500°C for 15 hours. To do this, we used one-dimensional photonic crystal (PhC) to trap the corresponding photon. It is well known that a PhC structure can manipulate light flow [27] due to the existence of the so-called photonic band gap (PBG) which prevent light to propagate in specific direction. Interestingly, when a defect layer is introduced into the PhC it will lead to the occurrence of the so-called photonic pass band (PPB) that allows a narrow window of light transmission in the corresponding PBG [28].

The CSD method was employed in this research due to its advantages, such as relatively low processing temperature, homogeneity composition, precise control of composition, and large area deposition [15, 24]. In addition, it also offers other advantages such as stoichiometry control, homogeneity, and low sintering temperature, and the most important is relatively low cost. These advantages are suitable for scientific research and development.

As the substrate layer we considered a one-dimensional PhC with a defect that consists of two different dielectric materials in a unit cell and a single defect layer in one of the unit cell. This treatment is expected to improve the sunlight absorbance. It was shown that the utilization of PhC on silicon solar cells can enhance photon absorption ranging from 15% to 26% depending on the associated PhC structures [29–32].

In this research, the combination of BST thin film with varying mole fraction and one-dimensional PhC is studied. It is found that a remarkable enhancement can be achieved. This report aims to discuss the results.

2. Experimental Methods

Instruments used in this research are analytical balance Sartonius model SL6100, ultrasonic Branson model 2210, spin coater reactor, LCR meter (HIOKI 3522-50 LCR Hitester), and VIS-NIR spectrophotometer ocean optics. The materials are barium acetate [$Ba(CH_3COO)_2$, 99%], strontium acetate [$Sr(CH_3COO)_2$, 99%], titanium isopropoxide [$Ti(C_{12}O_4H_{28})$, 99.999%], gallium trioxide [Ga_2O_3], 2-methoxyethanol [$H_3COOCH_2CH_2OH$, 99%], ethanol 96%, TCO glass, distilled water, silver paste, preparate glass, and aluminum foil. All these materials are from Sigma Aldrich.

As the first step in BST thin-film manufacturing, we prepared substrate of transparent conductive oxide (TCO); after that BST solution is made by reacting barium acetate, strontium acetate, titanium isopropoxide, and 5 mL of 2-methoxyethanol solvent using Branson Model 2210 ultrasonic for 90 minutes. Besides BST solution, BGST solution is made in the same way as BST solution, plus adding gallium oxide at 10% of the mass of BST. BGST and BST solutions are used as p-type and n-type layers, respectively. Next step is film growth processing; in this step, p-type layer manufacturing is done first then n-type layer. P-type layer (BGST solution) is grown by using spin coating reactor with speed of 6000 rpm for 30 seconds. For the n-type growth, its process is similar as p-type growth, but it is done after the p-type layer has been annealed.

The two last steps are annealing process and contact installation using aluminium metallization process. Annealing process, which aims to diffuse BST solution to substrate, is conducted at temperature of 500°C with increasing rate of 1.67°C/minutes and held up for 15 hours. The BST thin-film structure with photonic crystals layer is shown in Figure 1.

The optical characterizations of BST thin film, which are performed by using VIS-NIR optical spectroscopy ocean optics DT-mini-2 model, include measurements and calculations of absorbance, transmittance, absorbance coefficient, and attenuation coefficient. The setup processing of optical characterization is shown in Figure 2. While the electrical characterizations, that is, electrical conductivity, was carried out by measuring electrical conductance using LCR meter HIOKI 3522-50 LCR HiTester type, conductance measurements of these thin films were done at frequency of 100 kHz. The setup processing of electrical conductance characterization is shown in Figure 3.

3. Results and Discussions

3.1. Absorbance and Transmittance. The optical characterizations of BST thin film are performed in the wavelength of 400–800 nm. Absorbance (A), transmittance (T), and reflectance (R) values are expressed in percentage. The absorbance percentage is obtained based on the relationship that the total amount of absorbance, transmittance, and reflectance is equal to one ($A + T + R = 1$).

Figure 4(a) shows that the overall absorbance percentage of BST thin film has light absorption almost in every visible light spectrum range, even in the infrared region with absorption value more than 67.6%. In addition, it is indicated that the maximum absorbance of BST thin film for all barium mole fractions is in the range of 457 nm $\leq \lambda \leq$ 570 nm, and the minimum absorbance spectrum is in 570 nm $\leq \lambda \leq$ 678 nm. The largest absorbance was found at mole fraction $x = 0.25$ with average absorbance value of 92.04% and maximum and minimum absorbance peaks at wavelength of 502.7623 nm and 657.7201 nm, respectively. For $x = 0.35$, average absorbance value decreased to 83.55% with maximum and minimum peaks at wavelength of 506.4238 nm and 613.6818 nm, respectively. Then, absorbance value is increased to 91.16% at $x = 0.45$ with maximum and minimum absorbance peaks at 507.7586 nm and 618.5747 nm, respectively. For $x = 0.55$, overall average absorbance decreased to 80.12% with maximum and minimum absorbance peaks at 512.7549 nm and 608.7889 nm, respectively. Minimum absorbance value implies that electron did not absorb the photon energy. This means that most of them are transmitted or reflected.

Figure 4(b) shows that maximum absorbance value has the lowest transmittance value at $x = 0.25$ with overall average transmittance value of 3.79% with maximum transmittance peaks at 462.7919 and 657.7201 nm and minimum at 502.7623 nm. For $x = 0.35$, the overall average transmittance value is 8.25% with maximum transmittance peaks at

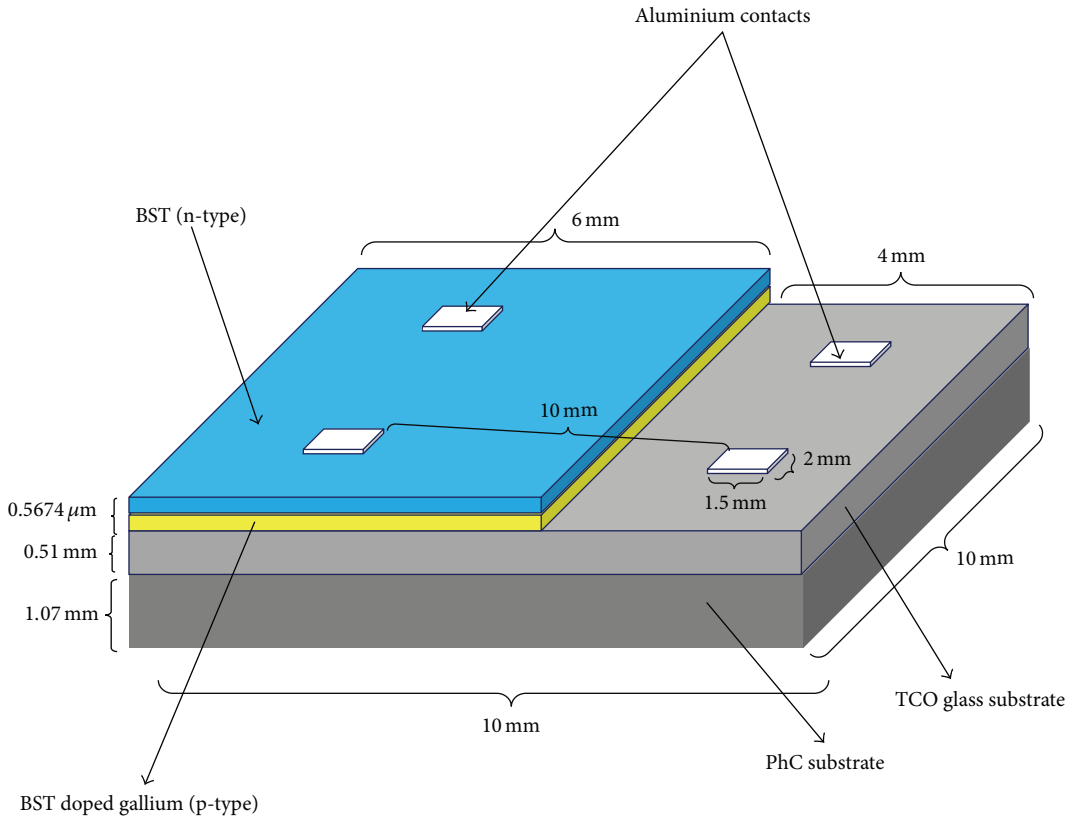

Figure 1: Structure of BST thin films with one-dimensional photonic crystal substrate.

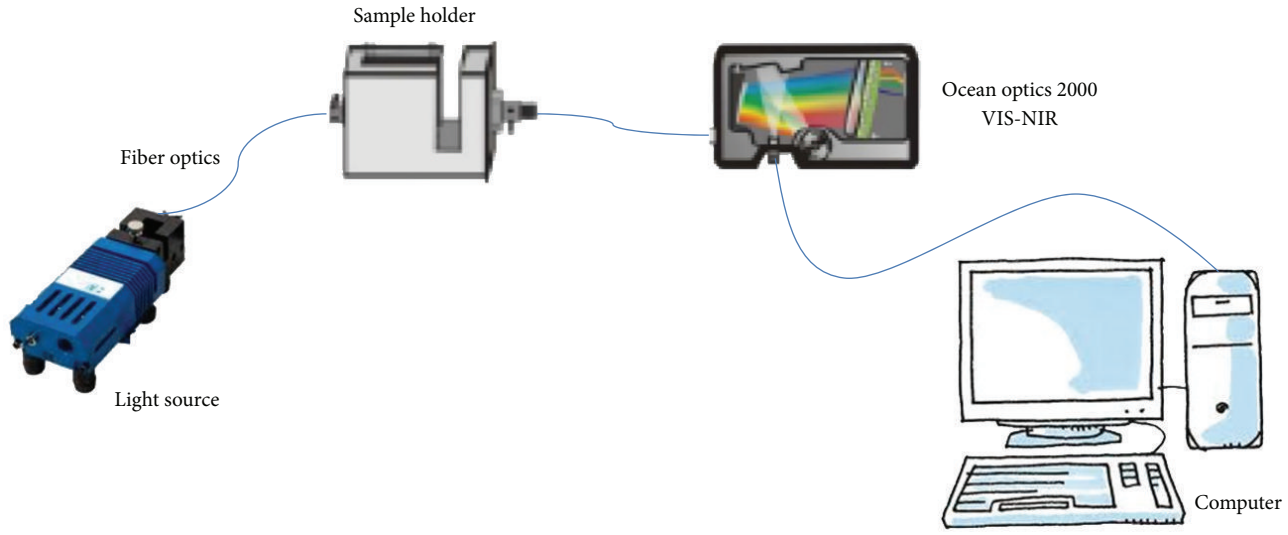

Figure 2: Setup of optical characterization.

445.9323 nm and 613.6818 nm and minimum at 507.7586 nm. Then, for $x = 0.55$, the overall transmittance value is 9.88% with maximum transmittance peaks at 442.8061 and 608.7889 nm, and minimum at 512.7549 nm.

It is shown that the addition of barium mole fraction leads to the increase of maximum absorbance or minimum transmittance peaks on the same light spectrum, that is, green. However, minimum absorbance or maximum transmittance is decreased, in the blue and red spectrum. These facts are due to the addition of barium moles which increased the atomic core radius which implies in the decrease of absorbance value of BST film. These can also be influenced by the increase of transmittance value (Table 1).

Besides absorbance and transmittance values, we also measured the reflectance value. As shown in Figure 5, it can be seen that the reflectance value is not significantly different

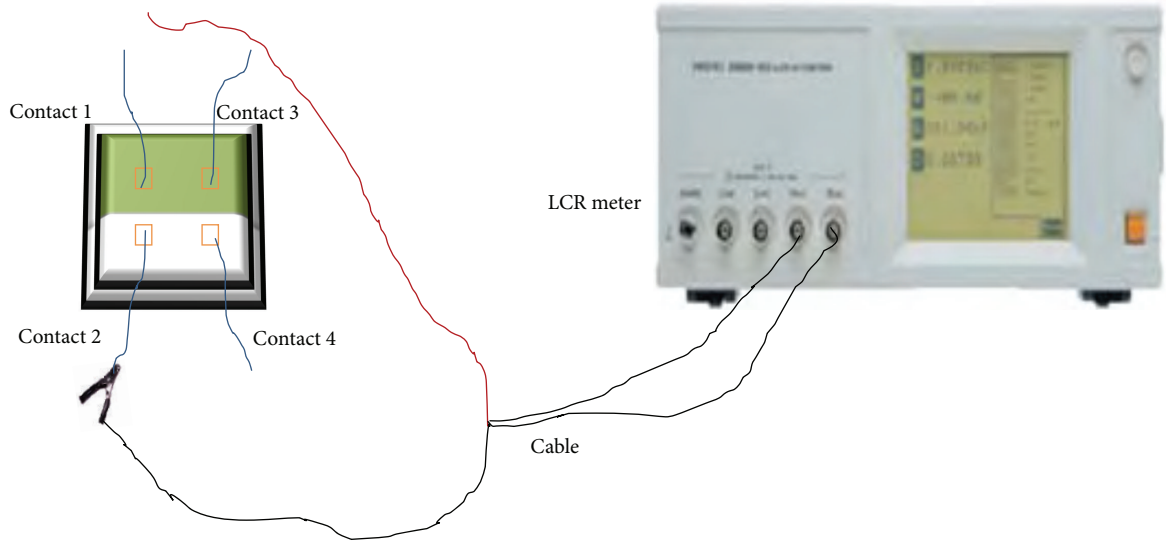

Figure 3: Setup of electrical conductance characterization.

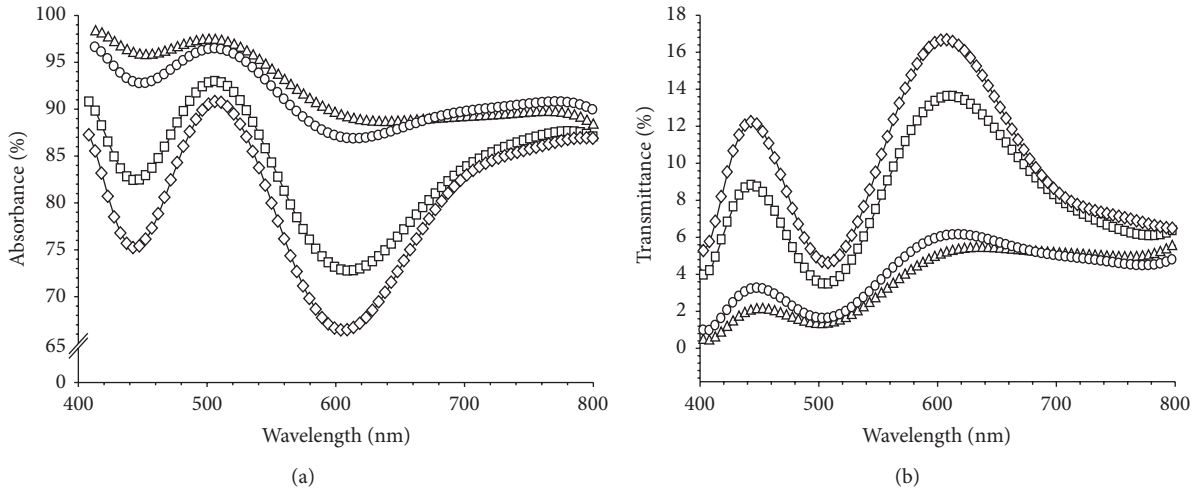

Figure 4: Relation between wavelength and (a) absorbance; (b) transmittance of BST thin films for mole fractions $x = 0.25$ (—Δ—), $x = 0.35$ (—□—), $x = 0.45$ (—○—), and $x = 0.55$ (—◊—).

from the transmittance and shares similar maximum and minimum reflectance peak patterns but with different values. This is consistent with the theory that when a material has the maximum absorbance value, so the transmittance and reflectance are minimum. Based on the average absorbance value more than 80.12% or the average transmittance and reflectance values less than 10% indicates that BST material which is employed in this study can be utilized as a material in the solar cell manufacturing, because one of the requirements of solar cell material is antireflective material [1, 7].

The PhC with defect that is used in this study as the BST thin-film substrate consists of 11 unit cells with each composed of two different dielectric materials of high and low refractive indices, namely, OS-5 (alloy of ZrO_2 and TiO_2) and MgF_2 with refractive indices of 2.1 and 1.38, respectively, and it was fabricated using electron beam evaporation method on substrate of standard glass material *borosilicate crown* (known as BK-7) with a refractive index of 1.52. Details of this fabricated PhC can be found in [33]. We inserted a single defect layer with different thickness in the related PhC such that a PPB occurred inside the associated PBG. Based on the results of UV-VIS spectroscopic measurements, as shown in Figure 6, the range of 400–612 nm corresponds to PBG of PhC, with the localized PPB transmittance being around 510.5300 nm.

When a polychromatic light is exposed to BST thin film with the embedded PhC, a part of light with specific wavelength is absorbed and transmitted by BST layer. However, there is a part of polychromatic light which is directly exposed to the PhC, especially on substrate surface which is not coated by BST. The light which is directly exposed to the surface of PhC and light with specific wavelength which is transmitted by BST layer are reflected back by PhC to BST. The total light spectra which are reflected by the PhC layer are then absorbed

Table 1: The shift of maximum and minimum absorbance and transmittance wavelengths of BST film caused by addition of barriums mole fraction.

Mole fraction (x)	Wavelength, λ (nm)	
	Absorbance	Transmittance
0.25	502.7623[a]	462.7919[a] dan 657.7201[a]
	657.7201[b]	502.7623[b]
0.35	506.4238[a]	445.9323[a] dan 613.6818[a]
	613.6818[b]	506.4238[b]
0.45	507.7586[a]	452.7993[a] dan 618.5747[a]
	618.5747[b]	507.7586[b]
0.55	512.7549[a]	442.8061[a] dan 608.7889[a]
	608.7889[b]	512.7549[b]

[a]Maximum absorption peak; [b]minimum absorption peak.

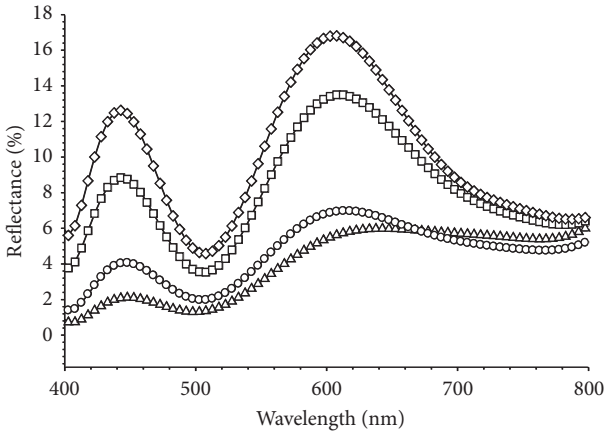

Figure 5: Relation between wavelength and reflectance value of BST thin films for mole fractions, $x = 0.25$ (—Δ—), $x = 0.35$ (—□—), $x = 0.45$ (—○—), and $x = 0.55$ (—◊—).

again by BST layer, so the absorbed light by BST is expected to be increased.

Significant changes in absorbance occurred when the PhC is applied to the associated BST thin-film. As shown in Figure 7, our BST thin film with embedded PhC shows increasing absorption for all x values in the range of 3.04% to 13.33%. For $x = 0.25$, the overall average absorbance percentage increased by 3.96% from 92.4% into 95.68% (Figure 7(a)). For $x = 0.35$, the average absorbance percentage increased by 7.07% into 89.45% from 83.55% (Figure 7(b)). Furthermore, the overall average absorbance at $x = 0.45$ increases from the 91.16% to 93.93% or increased only by 3.04% which is the lowest (Figure 7(c)), and $x = 0.55$ has the highest average absorbance percentage, that is, by 13.33% from 80.13% into 90.81%. (Figure 7(d)).

The largest absorbance was found at the mole fraction $x = 0.55$ with the highest being in orange spectrum (37.71%), followed by yellow spectrum which is 33.53%. Next, there are purple, red, blue, and green spectra with the amount of 17.85%, 12.32%, 11.24%, and 9.96%, respectively, while the lowest absorbance occurred at $x = 0.25$ except red spectrum (for $x = 0.45$). The lowest absorbance percentage is in purple

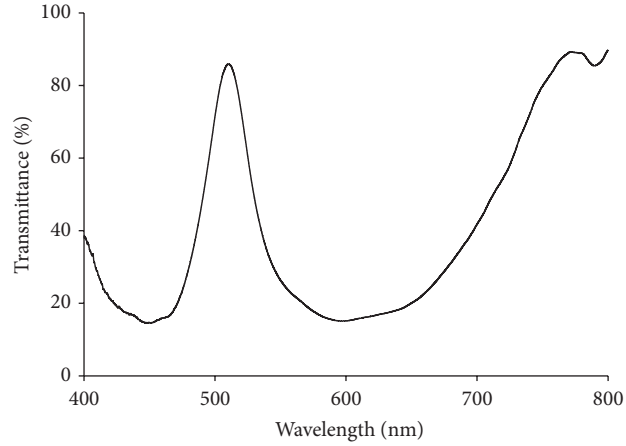

Figure 6: Comparison between absorbance of BST thin films with (—○—) and without (—Δ—) photonic crystals for mole fraction (a) $x = 0.25$, (b) $x = 0.35$ (c) $x = 0.45$, and (d) $x = 0.55$.

spectrum with an increase of only 0.39% followed by blue, green, red, yellow, and orange spectra with the amount of 0.87%, 2.08%, 2.55%, 6.44%, and 7.03%, respectively.

Higher absorbance of BST thin films, which is expressed in a percentage and varies for each x mole fraction, when compared to thin films without photonic crystals layer, is due to structure and characterization of photonic crystals layer. Remarkably, an almost flat absorbance feature in range of 400 to 700 nm was exhibited as shown in Figure 7, especially for $x = 0.45$. This interesting feature can be explained as the result of mutual combination between BST thin-film absorbance characteristic and transmittance of PhC given in Figure 6.

3.2. Attenuation Constant (k). It is well known that when light with specific wavelength illuminates a material, the corresponding intensity will be attenuated on short distance. In this condition, the wave's amplitude will decrease exponentially, with different intensity reduction for each material [34]. One of the parameters which is used to determine the attenuation effect is from its attenuation constant (k). By using (1), the value of k in this study can be determined from the following relation [35]:

$$\alpha = \frac{4\pi k}{\lambda}, \tag{1}$$

where k is attenuation constant value, λ is wavelength (m), and α is absorbance coefficient (cm^{-1}) which is obtained from the transmittance data using the following equation:

$$\alpha = \frac{\ln(1/T)}{d}, \tag{2}$$

where T is amount of transmittance and d is the thickness of BST films layer; in this study $d = 0.576\ \mu$m, which is obtained by using volumetric method.

Figures 8(a) and 8(b) show attenuation constant as a wavelength function of BST thin films with and without

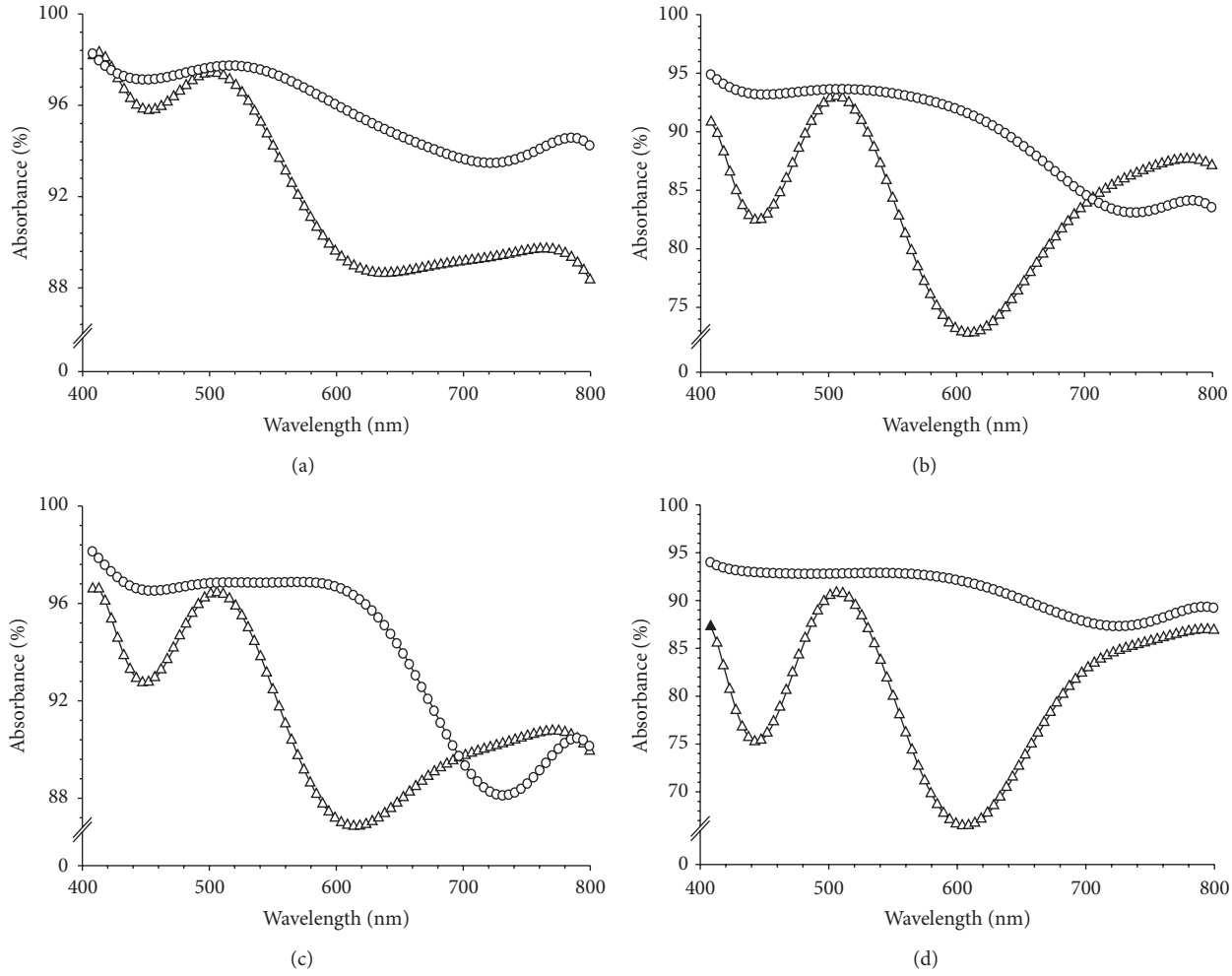

Figure 7: The transmittance value of PhC showing the PBG and the associated PPB.

photonic crystals layer. From these figures it can be seen that the attenuation constant value at particular wavelength indicates the amount of light energy which is absorbed or transmitted by those wavelengths.

3.3. Electrical Conductivity. The electrical conductivity of the corresponding BST thin film was obtained from the calculation using the following equation:

$$\sigma = \frac{Gl}{A}, \tag{3}$$

where σ is electrical conductivity value (S/cm), G is conductance value (S), l is distance between contacts (cm), and A is contact surface area (cm^2).

By using vernier caliper, values of the distance between contacts, length, and width contact which we obtained are 2.50 mm, 1.50 mm and 2.00 mm respectively. Then values of the thickness of TCO glass substrate and photonic crystals which we obtained are 0.51 mm and 1.07 mm, respectively, by using micrometer screw. Structure of BST thin film with PhC layer is given in Figure 1.

From characterization, we found that the corresponding electrical conductivity is in the range of 5.71250×10^{-2}–0.22525×10^{-1} S/cm. When referring to several literatures that classify materials based on their electrical conductivity, semiconductor materials are in the range of 10^{-8}–10^{3} S/cm [36]. By comparing these ranges of our BST and semiconductor materials, this BST thin film can be classified into semiconductor materials.

Characterizations which were performed at frequency of 100 kHz show that the larger barium mole fraction leads to the higher electrical conductivity of BST thin film with nonlinear tendency, and when it is exposed to the light, its electrical conductivity is decreased (Table 2). This phenomenon occurred due to electron-hole recombination process within semiconductor materials which reduce electron concentration as charge carriers in conduction band [9].

4. Conclusion

The optical characterizations show that the overall absorbance percentage of the considered BST thin film has light absorption area on almost the entire range of

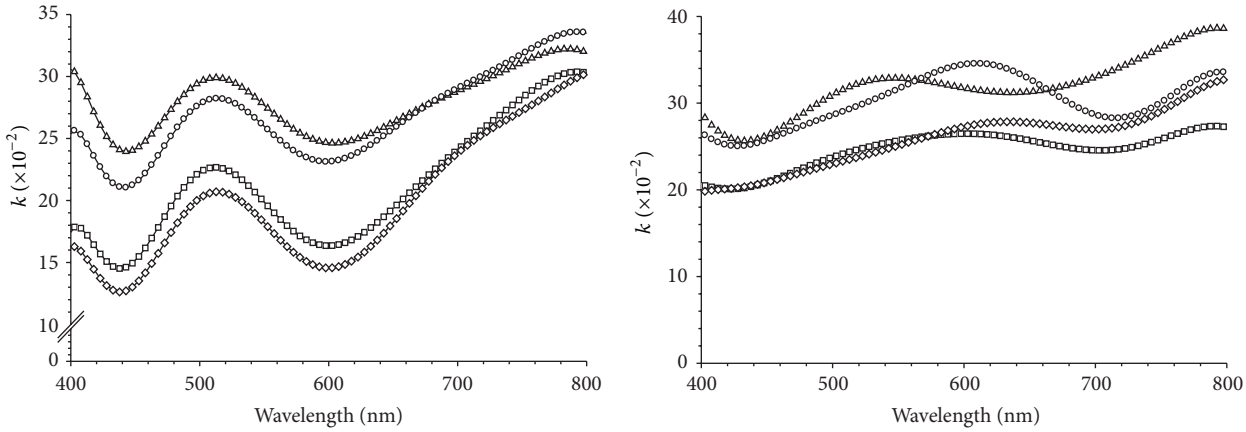

Figure 8: Relation between wavelength and attenuation constant of BST thin films without (a) and with (b) photonic crystals for mole fraction $x = 0.25$ (—Δ—), $x = 0.35$ (—□—), $x = 0.45$ (—○—) and $x = 0.55$ (—◊—).

Table 2: Electrical conductivity value (σ) of BST thin films after exposed by light with intensity more than 2000 lux (bright condition).

Mole fraction (x)	σ ($\times 10^{-1}$ S/cm)				Reduction percentage σ (%)	
	Dark		Bright			
	A	B	A	B	A	B
0.25	0.57125	0.22525	0.24813	0.20508	130,22206	9,83519
0.35	5.10250	0.51025	3.25333	0.43117	56,83930	18,34079
0.45	4.96366	1.05475	1.21908	1.03142	307,16442	2,26193
0.55	3.50833	1.86517	2.10444	1.08008	66,71086	72,68813

Conducted relatively to mole fraction $x = 0.25$; A: without photonic crystals layer; B: with photonic crystals layer.

the visible light spectrum even to the infrared range with absorption value more than 67.6%. For $x = 0.25$, 0.35, 0.45, and 0.55 visible spectra have average absorption percentages of 92.04%, 83.55%, 91.16%, and 80.12%, respectively.

A significant change occurred when PhC substrate is embedded in BST thin film which shows increasing in photons absorption in the wavelength of 400–780 nm; those are 3.96%, 7.07%, 3.04%, and 13.33% for $x = 0.25$, 0.35, 0.45, and 0.55, respectively. A remarkable feature of almost flat absorbance characteristics was observed. This feature occurred due to mutual combination between BST thin film and the corresponding PhC with defect.

By considering solar cell material ability in absorbing photons, it can be concluded that the associated BST material can be further utilized as a solar cell material; however, further testing on other solar cell properties is required such as photovoltaic characteristics, fill factor, and efficiency scale in photon-to-current conversion process.

Conflict of Interests

The authors declare that there is no conflict of interests regarding the publication of the paper.

Acknowledgments

This work is supported by National Innovation System (SINas) Research Grant from the Ministry of Research and Technology, Republic of Indonesia, under contract no. 38/SEK/INSINAS/PPK/I/2013. Nuayi would like to thank the Ministry of Education and Culture, Republic of Indonesia, for his postgraduate funding through BPPS scholarship.

References

[1] R. H. Bossert, C. J. J. Tool, J. A. M. van Roosmalen, C. H. M. Wentink, and M. J. M. de Vaan, "Thin-film solar cells, technology evaluation and perspectives," Tech. Rep., 2000, http://citeseerx.ist.psu.edu/viewdoc/download?doi=10.1.1.196.7245&rep=rep1&type=pdf.

[2] K. L. Chopra, P. D. Paulson, and V. Dutta, "Thin-film solar cells: an overview," *Progress in Photovoltaics*, vol. 12, no. 2-3, pp. 69–92, 2004.

[3] Y. Guo, L. Huang, and A. L. Porter, "The research profiling method applied to nano-enhanced, thin-film solar cells," *R & D Management*, vol. 40, no. 2, pp. 195–208, 2010.

[4] T. V. Torchynska and G. Polupan, "High efficiency solar cell for space applications," *Superficies y Vacío*, vol. 17, pp. 21–25, 2004.

[5] R. B. Bergmann, "Crystalline Si thin-film solar cells: a review," *Applied Physics A*, vol. 69, no. 2, pp. 187–194, 1999.

[6] A. G. Aberle, "Thin-film solar cells," *Thin Solid Films*, vol. 517, no. 17, pp. 4706–4710, 2009.

[7] W. W. Wenas, "Teknologi sel surya: Perkembangan dewasa ini dan yang akan datang," 2004, http://www.energi.lipi.go.id/.

[8] J. W. Kim, T. Osumi, M. Mastuoka et al., "Preparation and characterization of $Ba(Zr_xTi_{1-x})O_3$ thin films using reactive sputtering method," *Japanese Journal of Applied Physics*, vol. 51, pp. 1–5, 2012.

[9] Irzaman, "Studi fotodiode film tipis semikonduktor $Ba_{0,6}Sr_{0,4}TiO_3$ didadah tantalum," *Jurnal Sains Material Indonesia*, vol. 10, pp. 18–22, 2008.

[10] Irzaman, A. Arif, H. Syafutra, and M. Romzie, "Studi konduktivitas listrik, kurva I-V, dan celah energi fotodioda berbasis film tipis semikonduktor $Ba_{0,75}Sr_{0,25}TiO_3$ (BST) yang didadah galium (BST) menggunakan metode chemical solution deposition (CSD)," *Jurnal Aplikasi Fisika*, vol. 5, pp. 22–30, 2009.

[11] A. Ioachim, M. I. Toacsan, L. Nedelcu et al., "Dielectric properties of (Ba,Sr)TiO_3 thin films for applications in electronics," *Romanian Journalof Information Science and Technology*, vol. 10, pp. 347–354, 2007.

[12] F. M. Pontes, E. R. Leite, D. S. L. Pontes et al., "Ferroelectric and optical properties of $Ba_{0.8}Sr_{0.2}TiO_3$ thin film," *Journal of Applied Physics*, vol. 91, no. 9, pp. 5972–5978, 2002.

[13] F. Fitsilis, S. Regnery, P. Ehrhart et al., "BST thin films grown in a multiwafer MOCVD reactor," *Journal of the European Ceramic Society*, vol. 21, no. 10-11, pp. 1547–1551, 2001.

[14] S. B. Singh, H. B. Sharma, H. N. K. Sarma, and S. Phanjoubam, "Optical and structural properties of nano-sized barium strontium titanate ($Ba_{0.6}Sr_{0.4}TiO_3$) thin film," *Modern Physics Letters B*, vol. 22, no. 9, pp. 693–700, 2008.

[15] Y. Xin, R. Wei, S. Peng, W. Xiaoqing, and Y. Xi, "Enhanced tunable dielectric properties of $Ba_{0.5}Sr_{0.5}TiO_3/Bi_{1.5}Zn_{1.0}Nb_{1.5}O_7$ multilayer thin films by a sol-gel process," *Thin Solid Films*, vol. 520, no. 2, pp. 789–792, 2011.

[16] N. B. Ibrahim, E. Yusrianto, Z. Zalita, and Z. Ibarahim, "Effect of annealing temperature of Sol-Gel TiO_2 buffer layer on microstructure and electrical properties of $Ba_{0.6}Sr_{0.4}TiO_3$ films," *Sains Malaysiana*, vol. 41, no. 3, pp. 339–344, 2012.

[17] K. Verma, S. Sharma, D. K. Sharma, R. Kumar, and R. Rai, "Sol gel processing and characterization of nanometersized (Ba, Sr)TiO_3 ceramics," *Advanced Materials Letters*, vol. 3, pp. 44–49, 2012.

[18] M. Tyunina, M. Plekh, J. Levoska et al., "Dielectric properties of atomic layer deposited thin-film barium strontium titanate," *Integrated Ferroelectrics*, vol. 102, no. 1, pp. 29–36, 2008.

[19] D. Gao, D. Xiao, J. Bi et al., "Hydrothermal syntheses of barium strontium titanate thin films," *Materials Transactions*, vol. 44, no. 7, pp. 1320–1323, 2003.

[20] I. P. Koutsaroff, A. Kassam, M. Zelner et al., "Dielectric properties of (Ba,Sr)TiO_3 thin film capacitors fabricated on alumina substrates," *MRS Proceedings*, vol. 748, article U6.1, 2003.

[21] P. M. Suherman, Y. Y. Tse, T. J. Jackson et al., "Comparison of structural, microstructural, and electrical analyses of barium strontium titanate thin films," *Journal of Applied Physics*, vol. 105, no. 6, Article ID 061604, 2009.

[22] Y. Iriani, M. Hikam, B. Soegijono, and I. Mudzakir, "Pengaruh heating rate dan jumlah lapisan terhadap sifat listrik (kurva histeresis) pada lapisan tipis Barium Strontium Titanat," *Indonesian Journal of Materials Science*, pp. 205–208, 2008.

[23] Irzaman, A. Marwan, A. Arief, R. A. Hamdani, and M. Komaro, "Electrical conductivity and surface rougness properties of ferroelectric gallium doped $Ba_{0.5}Sr_{0.5}TiO_3$ (BGST) thin film," *Indonesian Journal of Physics*, vol. 19, pp. 119–121, 2008.

[24] Irzaman, H. Syafutra, H. Darmasetiawan et al., "Electrical properties of photodiode $Ba_{0.25}Sr_{0.75}TiO_3$ (BST) thin film doped with ferric oxide on p-type Si (100) substrate using chemical solution deposition method," *Atom Indonesia*, vol. 37, pp. 133–138, 2011.

[25] N. Sirikulrat, "Colossal dielectric constant and a microfarad tunable capacitance in platinum thin film-antimony doped Barium Strontium Titanate Schottky barrier diodes," *Thin Solid Films*, vol. 520, no. 1, pp. 633–640, 2011.

[26] S. M. Aygün, J. F. Ihlefeld, W. J. Borland, and J.-P. Maria, "Permittivity scaling in $Ba_{1-x}Sr_xTiO_3$ thin films and ceramics," *Journal of Applied Physics*, vol. 109, no. 3, Article ID 034108, 2011.

[27] J. D. Joannopoulos, S. G. Johnson, J. N. Winn, and R. D. Meade, *Photonic Crystal: Molding the Flow of Light*, Princeton University Press, Princeton, NJ, USA, 2008.

[28] H. Alatas, H. Mayditia, H. Hardhienata, A. A. Iskandar, and M. O. Tjia, "Single-frequency refractive index sensor based on a finite one-dimensional photonic crystals with two defects," *Japanese Journal of Applied Physics*, vol. 45, pp. 6754–6758, 2006.

[29] P. Bermel, C. Luo, L. Zeng, L. C. Kimerling, and J. D. Joannopoulos, "Improving thin-film crystalline silicon solar cell efficiencies with photonic crystals," *Optics Express*, vol. 15, no. 25, pp. 16986–17000, 2007.

[30] A. Chutinan, N. P. Kherani, and S. Zukotynski, "High-efficiency photonic crystal solar cell architecture," *Optics Express*, vol. 17, no. 11, pp. 8871–8878, 2009.

[31] Y. Park, E. Drouard, O. E. Daif et al., "Absorption enhancement using photonic crystals for silicon thin film solar cells," *Optics Express*, vol. 17, no. 16, pp. 14312–14321, 2009.

[32] A. Deinega and S. John, "Solar power conversion efficiency in modulated silicon nanowire photonic crystals," *Journal of Applied Physics*, vol. 112, no. 7, Article ID 074327, 2012.

[33] W. Maulina, M. Rahmat, E. Rustami et al., "Fabrication and characterization of NO_2 gas sensor based on one dimensional photonic crystal for measurement of air pollution index," in *Proceedings of the 2nd International Conference on Instrumentation, Communication, Information Technology and Biomedical Engineering (ICICI-BME '11)*, pp. 352–355, Bandung, Indonesia, November 2011.

[34] A. Maddu and G. E. Timuda, "Pengaruh ketebalan terhadap sifat optik lapisan semikonduktor Cu_2O yang dideposisikan dengan metode chemical bath deposition (CBD)," *Jurnal Ilmu Pengetahuan dan Teknologi Telaah*, vol. 28, pp. 1–5, 2010.

[35] W. J. Leng, C. R. Yang, J. H. Zhang et al., "Structural and optical properties of $Ba_xSr1_{-x}TiO_3$ thin films on indium tin oxide/quartz substrates prepared by radio-frequency magnetron sputtering," *Journal of Applied Physics*, vol. 99, no. 11, Article ID 114904, pp. 1–5, 2006.

[36] K. K. Ng, *Complete Guide to Semiconductor Device*, McGraw-Hill, New York, NY, USA, 1995.